JOURNAL OF BACTERIOLOGY, Nov. 2007, p. 8257–8269 Vol. 189, No. 22
0021-9193/07/$08.00+0 doi:10.1128/JB.00645-07

New Insights into the WalK/WalR (YycG/YycF) Essential Signal Transduction Pathway Reveal a Major Role in Controlling Cell Wall Metabolism and Biofilm Formation in *Staphylococcus aureus*▽

Sarah Dubrac,[1] Ivo Gomperts Boneca,[2] Olivier Poupel,[1] and Tarek Msadek[1]*

Unité de Biologie des Bactéries Pathogènes à Gram Positif, CNRS URA 2172, Institut Pasteur, 25 rue du Dr. Roux, 75724 Paris Cedex 15, France,[1] and Unité de Pathogénie Bactérienne des Muqueuses, Institut Pasteur, 28 rue du Dr. Roux, 75724 Paris Cedex 15, France[2]

Received 24 April 2007/Accepted 28 August 2007

The highly conserved WalK/WalR (also known as YycG/YycF) two-component system is specific to low-G+C gram-positive bacteria. While this system is essential for cell viability, both the nature of its regulon and its physiological role have remained mostly uncharacterized. We observed that, unexpectedly, *Staphylococcus aureus* cell death induced by WalKR depletion was not followed by lysis. We show that WalKR positively controls autolytic activity, in particular that of the two major *S. aureus* autolysins, AtlA and LytM. By using our previously characterized consensus WalR binding site and carefully reexamining the genome annotations, we identified nine genes potentially belonging to the WalKR regulon that appeared to be involved in *S. aureus* cell wall degradation. Expression of all of these genes was positively controlled by WalKR levels in the cell, leading to high resistance to Triton X-100-induced lysis when the cells were starved for WalKR. Cells lacking WalKR were also more resistant to lysostaphin-induced lysis, suggesting modifications in cell wall structure. Indeed, lowered levels of WalKR led to a significant decrease in peptidoglycan biosynthesis and turnover and to cell wall modifications, which included increased peptidoglycan cross-linking and glycan chain length. We also demonstrated a direct relationship between WalKR levels and the ability to form biofilms. This is the first example in *S. aureus* of a regulatory system positively controlling autolysin synthesis and biofilm formation. Taken together, our results now define this signal transduction pathway as a master regulatory system for cell wall metabolism, which we have accordingly renamed WalK/WalR to reflect its true function.

Staphylococcus aureus, a major gram-positive pathogen, is a leading cause of both hospital- and community-acquired infections. *S. aureus* is responsible for a wide spectrum of diseases, ranging from superficial skin infections to life-threatening septicemia, endocarditis, and pneumonia. This tenacious pathogen has rapidly emerged as a major public health threat through the increased appearance of drug-resistant isolates, particularly methicillin- and vancomycin-resistant strain (MRSA and VRSA) often resulting in the inability to treat certain infections (46).

S. aureus is a widespread bacterium that can persist through asymptomatic carriage either as a commensal of the human nose, in 30 to 70% of the population, or as part of the epidermal flora, factors favoring dissemination of *S. aureus* infections (9, 55). *S. aureus* can also survive outside the host in various environments, such as water and soil. Recognition of environmental signals enables *S. aureus* to adapt by coordinating gene expression to survive a diverse range of stresses. Two-component systems (TCSs) are integrative signal transduction regulatory pathways composed of a sensing module, a histidine kinase, and its cognate transcription regulator. TCSs are key components allowing adaptation of bacterial metabolism to various environments. Genome scanning has predicted 17 potential TCSs in *S. aureus*, some of which have been reported to be regulators of bacterial virulence. The AgrCA TCS is a well-known global regulatory system controlling numerous genes involved in *S. aureus* virulence, such as cytotoxin- and hemolysin-encoding genes, but other TCSs, such as ArlSR, SaeSR, VraSR, and SsrAB, have also been reported to play roles in *S. aureus* virulence (2, 32, 41).

While TCSs are regulatory systems responsible for bacterial fitness under certain stress conditions, few to date have been shown to be essential for cell viability. Among these, the WalK/WalR (also known as YycG/YycF) TCS is highly conserved and specific to low-G+C gram-positive bacteria. It has been shown, or is thought, to be essential in *Bacillus subtilis*, *S. aureus*, *Enterococcus faecalis*, *Listeria monocytogenes*, *Streptococcus pneumoniae*, and *Streptococcus mutans* (13, 15, 20, 22, 30, 33, 36, 49).

The first two genes of the *yycFG* operon encode the WalKR TCS. Interestingly, within the phylum *Firmicutes*, the structural organization of this operon varies significantly between the different orders of the class *Bacillus*. In the order *Bacillales*, as well as in most of the *Lactobacillales*, the operon contains several additional genes, six in total for *B. subtilis* and the family *Listeriaceae* (*yycFGHIJ yyxA*) but only five in the family *Staphylococcaceae*, in which the last gene, *yyxA*, encoding an HtrA-like protease, is missing. In contrast, in members of the order *Streptococcaceae*, the operon is limited to only three

* Corresponding author. Mailing address: Unité de Biologie des Bactéries Pathogènes à Gram Positif, Institut Pasteur, 25 rue du Dr. Roux, 75724 Paris Cedex 15, France. Phone: (33) 1 45 68 88 09. Fax: (33) 1 45 68 89 38. E-mail: tmsadek@pasteur.fr.

▽ Published ahead of print on 7 September 2007.

genes, *yycFGJ*. The reason for the essential nature of this TCS remains elusive in most bacteria, except for *S. pneumoniae*, in which WalKR-dependent expression of *pcsB* is required for cell viability (39, 40). PcsB (Spr2021) is a CHAP (cysteine, histidine-dependent amidohydrolase/peptidase) domain protein that is essential in *S. pneumoniae* and has been shown to be involved in cell wall synthesis (39). Expression profiling of *S. pneumoniae* cells starved for WalKR revealed that the TCS controls additional genes encoding potential cell wall-associated proteins (40).

In *B. subtilis*, we have previously shown that the WalR response regulator binds specifically in vitro to the promoter regions of four genes involved in cell wall metabolism: *yocH* and *ykvT*, encoding potential cell wall hydrolyases, as well as *tagAD*, whose products are key enzymes of teichoic acid biosynthesis (26). In *S. aureus*, the viability of a *yycF* thermosensitive mutant under nonpermissive conditions was restored by high sucrose and NaCl concentrations, suggesting a role for the WalKR TCS in the regulation of cell wall structure (36). During our previous studies of the WalKR TCS of *S. aureus* (13), we showed that WalR binds specifically in vitro to the promoter regions of *lytM*, encoding a major autolysin, as well as *ssaA* and *isaA*, which as we show here encode proteins potentially involved in peptidoglycan hydrolysis.

The effect of the WalKR TCS on cell wall metabolism has not been specifically studied. Our interest in this subject was initiated by the following observation: while the absence of this TCS in *S. aureus* is lethal, there is no cell lysis after bacterial death. We show here that the activities of the two major *S. aureus* autolysins, AtlA and LytM, are positively controlled by the WalKR TCS. These results are correlated with transcriptional activation of *atlA* and *lytM*, as well as several additional genes encoding potential cell wall-hydrolytic enzymes. Further investigation of the influence of the WalKR TCS on peptidoglycan composition allowed us to show that lowered levels of WalKR led to increases in peptidoglycan cross-linking and glycan chain length. We also show that peptidoglycan biosynthesis and turnover rates are significantly lowered under conditions of WalKR depletion. Additionally, we demonstrate a direct relationship between WalKR levels in the cell and the ability to form biofilms. This is the first example in *S. aureus* of a TCS positively controlling autolysin synthesis and biofilm formation.

Taken together, results obtained with different bacteria clearly indicate that although the regulons controlled in the various members of the closely related low-G+C group of bacteria appear to be quite different, it is now clear that the WalKR TCS plays an essential role in cell wall metabolism. In order to standardize the nomenclature for this system in different bacteria and better reflect its true function, we suggest that it be henceforth referred to as WalK (histidine kinase) and WalR (response regulator).

MATERIALS AND METHODS

Bacterial strains and growth media. *S. aureus* strain ST1000 (RN4220 P*spac-yycF*) carries plasmid pSD3-3 (13), a derivative of pDH88 (25), integrated at the *yycFGHIJ* locus, placing the entire operon under the control of the P*spac* isopropyl-β-D-thiogalactopyranoside (IPTG)-inducible promoter. *S. aureus* strains were grown in Trypticase soy broth (TSB) supplemented with chloramphenicol (10 μg ml^{-1}).

Viability testing. Bacteria were stained using the LIVE/DEAD BacLight viability assay L-7012 (Molecular Probes-Invitrogen, Carlsbad, CA). This stain distinguishes live cells from dead bacteria based on membrane integrity and two nucleic acid stains. The green fluorochrome (SYTO 9) can penetrate intact membranes, while the larger red fluorochrome (propidium iodide) penetrates only compromised membranes of dead bacteria. Bacterial cultures were grown in TSB with or without IPTG (1 mM). At appropriate optical densities (ODs), the cultures were washed three times in phosphate-buffered saline (PBS) and concentrated in PBS between 2 and 10 times depending on the initial ODs. Staining and fluorescence microscopic observations were then carried out as specified by the manufacturer.

Zymographic analysis of bacteriolytic activities. Protein preparations, sodium dodecyl sulfate-polyacrylamide gel electrophoresis (SDS-PAGE), and detection of bacteriolytic activities were performed as previously described with some modifications (51). Briefly, SDS-extracted proteins were prepared from 50-ml cultures of strain ST1000 grown in TSB with or without IPTG (1 mM) to an OD at 600 nm (OD_{600}) of approximately 1 at 37°C with aeration (up to that point, cultures grown with and without IPTG had the same growth rate). Cells were harvested by centrifugation (10 min; 5,200 × *g*), and the pellets were resuspended in 1 ml of 2× Laemmli SDS sample buffer and heated for 5 min at 99°C. After centrifugation (10 min; 20,800 × *g*), 40 μl of supernatant containing SDS-soluble proteins was subjected to SDS-PAGE with heat-inactivated staphylococcal cells (equivalent to an OD_{600} of 10) as a substrate in the separation gel (10% acrylamide). Following electrophoresis, the gel was washed to remove the SDS and to allow protein refolding and incubated in phosphate buffer (0.1 M $NaPO_4$, pH 7) at 37°C. Protein bands with bacteriolytic activities were detected as clear zones in the opaque gel.

Peptidoglycan purification and structural analysis. ST1000 cells were grown in 500 ml of TSB with or without 1 mM IPTG, and the bacteria were harvested by centrifugation (10 min; 5,400 × *g*) at the time of cessation of growth in the absence of inducer (OD_{600}, ~1). The bacteria were rapidly incubated in an ice-ethanol bath, and peptidoglycan purification was carried out as previously described (10). Muropeptide composition and glycan strand length analyses were performed as previously described (5, 10), except that to generate free glycan strands, we used the recombinant amidase domain of AtlA (kindly provided by Simon Foster, University of Sheffield, Sheffield, United Kingdom). Amidase digestion of peptidoglycan was performed in 10 mM Tris-HCl, pH 7.5, 1 mM $CaCl_2$ at 37°C with stirring overnight.

Cell wall biosynthesis and turnover. For measuring cell wall biosynthesis, TSB medium containing 20 μM of *N*-acetyglucosamine (GlcNAc) and 0.1 μM of [^{3}H]GlcNAc (10 Ci/mmol) was inoculated with an overnight culture of strain ST1000 at an OD_{600} of 0.001 with 0.05 mM, 1 mM, or no IPTG. The cultures were incubated at 37°C with shaking, and aliquots (100 μl) were taken every 20 min for 3 h (approximately six generations) and immediately frozen at −20°C. At the end of the 3-h labeling period, cells from the 0.05 mM and 1 mM IPTG cultures were pelleted (10 min; 5,200 × *g*) and resuspended in prewarmed TSB containing 20 μM of unlabeled GlcNAc and either no IPTG (cells from the 0.05 mM labeling culture) or 1 mM IPTG (cells from the 1 mM labeling culture) to measure cell wall turnover. Aliquots (500 μl) were taken every 20 min over a 3-h period (about six generations) and immediately frozen at −20°C. Sample treatment and quantification were performed as previously described (11) with some modifications. Briefly, extracts were prepared by boiling samples in 4% SDS for 30 min and filtering them onto 0.22-μm nitrocellulose filters (Millipore). The filtered samples were then washed (once with 3 ml of 0.1 M LiCl and three times with 3 ml H_2O) before the retained radioactivity was measured.

Extraction of total RNA. Strain ST1000 was grown in TSB with IPTG (0.05 mM or 1 mM) at 37°C with aeration to an OD_{600} of 1.2. The cells were pelleted (2 min; 20,800 × *g*) and immediately frozen at −20°C. RNA extractions were then performed as previously described (7), followed by a DNase I treatment with the TURBO DNA-free reagent (Ambion, Austin, TX) in order to eliminate residual contaminating genomic DNA.

cDNA synthesis. Reverse transcription reaction mixtures (20 μl) containing 200 ng of random hexamers (Roche, Basel, Switzerland), 0.5 mM deoxynucleoside triphosphate, and 5 μg of total RNA were incubated at 65°C for 5 min to remove secondary structures and placed on ice. Avian myeloblastosis virus reverse transcriptase (25 U) and its buffer (Roche, Basel, Switzerland) were then added to the mixture. After 10 min at 25°C, the mixture was incubated at 42°C for 50 min. The reverse transcriptase was then inactivated by heating the mixture at 70°C for 15 min.

qRT-PCRs. Primers were selected with BEACON Designer 4.02 software (Premier Biosoft International, Palo Alto, CA) in order to design 200- to 300-bp amplicons (Table 1 shows the primer sequences). Quantitative real-time PCRs (qRT-PCRs) were performed in a 25-μl reaction volume containing 5 μl of a

TABLE 1. Primers used in this study

Gene	Primer name	Primer sequence
16S rRNA	OSA161	5′-ACGTGGATAACCTACCTATAAGACTGGGAT-3′
	OSA162	5′-TACCTTACCAACTAGCTAATGCAGCG-3′
yycG (SA0018)	OSA158	5′-TACAATCCCTTCATACTAAACTTGTAATTG-3′
	OSA159	5′-GTGCATTTACGGAGCCCTTTTCGTCATATAC-3′
sceD (SA1898)	OSA168	5′-GCAGTAGGTTTAGGAATCGTAGCAGGAAAT-3′
	OSA169	5′-CTGATTCAAAGTGATAAGTAAACCCTTCAT-3′
ssaA (SA2093)	OSA119	5′-CCGTACTGGTGGTTTAGGTGCAAGCTACAG-3′
	OSA120	5′-GCATTGCCCCAAGTTGAACCGATTTTACCA-3′
SA0620	OSA186	5′-CTTCTACACAACATACAGTACAAT-3′
	OSA187	5′-TCAACTGAAACACCATATCTGC-3′
SA2097	OSA188	5′-GATTCACAGTAAATCATACACCTTC-3′
	OSA189	5′-TGATGACATATGTACTAGAATTAAG-3′
SA2353	OSA196	5′-CATGATGCACAAGCCGCAGA-3′
	OSA197	5′-GATGCATTGTTATAACTATA-3′
SA0710	OSA209	5′-AATTATATTCATACAATCCTGGTG-3′
	OSA210	5′-GGTGCTTGCTTAACTACTAC-3′
isaA (SA2356)	OSA121	5′-GGTACTACATGGTCATGGAGCTATGAAGC-3′
	OSA122	5′-CTCACTGAACTTGAAGTAGTTGAAGTGCTG-3′
lytM (SA0265)[a]	OSA182	5′-CAGCAACAGCAGGAGATAAC-3′
	OSA183	5′-ATAATTGACCTTTCCATTACCATC-3′
lytM (SA0265)[b]	OSA90	5′-GAGAAGCATATCACTATTAGAAAGTTG-3′
	OSA91	5′-GCGCCATTGTAAATGTAGCGAAGCCC-3′
atlA (SA0905)	OSA203	5′-AACAGCACCAACGGATTAC-3′
	OSA204	5′-CATAGTCAGCATAGTTATTCATTG-3′

[a] Primers used for qRT-PCR.
[b] Primers used for primer extension experiments.

1/100 dilution of cDNA, 1 μl of gene-specific primers (10 μM), and 12.5 μl of iQ SYBR Green Supermix (Bio-Rad, Hercules, CA). PCR amplification, detection, and analysis were performed with the MyiQ Single-Color Real-Time iCycler PCR Detection System and the MyiQ Optical System Software (Bio-Rad, Hercules, CA). PCR conditions included an initial denaturation step at 95°C for 3 min, followed by a 40-cycle amplification (95°C for 15 s, 55°C for 15 s, and 72°C for 15 s). The specificity of the amplified product and the absence of primer dimer formation were verified by generating a melting curve with a final step of 80 cycles consisting of a stepwise 0.5°C temperature increase every 10 s, beginning at 55°C. The absence of contaminating genomic DNA was verified by testing each sample in control reactions without a prior reverse transcription step. The critical threshold cycle (C_T) was defined for each sample.

The expression levels of the tested genes were normalized using the 16S rRNA gene of *S. aureus* as an internal standard whose transcript level did not vary under our experimental conditions (Table 1 shows the primer sequences). Each assay was performed in quadruplicate and repeated with at least three independent RNA samples. The change (*n*-fold) in the transcript level was calculated using the following equations: $\Delta C_T = C_{T(\text{test DNA})} - C_{T(\text{reference cDNA})}$, $\Delta\Delta C_T = \Delta C_{T(\text{target gene})} - \Delta C_{T(16\text{S rRNA})}$, and ratio = $2^{-\Delta\Delta C_T}$ (35).

Primer extension reactions. Total RNA was used as the template for primer extension reactions using OSA91, a radiolabeled *lytM*-specific primer (Table 1), as previously described (7). The corresponding Sanger DNA-sequencing reactions were carried out by using the same primer and a PCR-amplified fragment containing the *lytM* upstream region (OSA90-OSA91) with the Sequenase PCR product sequencing kit (USB, Cleveland, OH).

Microscopy. For microscopic observations of bacterial morphology and organization, strain ST1000 was grown in TSB with or without 1 mM IPTG at 37°C under static conditions to an OD_{600} of ~1. The cells were then immobilized using agarose-coated microscope slides as previously described (38). Micrographs were taken under phase-contrast light microscopy at ×1,000 magnification.

Triton X-100 and lysostaphin lysis assays. Cultures of strain ST1000 in TSB with or without 1 mM IPTG were allowed to grow at 37°C with aeration to an OD_{600} of ~1 (just prior to the arrest of growth in the absence of inducer). Cells were harvested (10 min; 5,400 × *g*) and resuspended in the same volume of PBS (control) or PBS containing either 0.1% Triton X-100 or 200 ng/ml lysostaphin. These suspensions were then incubated at 30°C (Triton lysis assay) or 37°C (lysostaphin assay) with aeration. Lysis was determined as the decrease in the OD_{600} over time. The results were presented as percentage lysis, calculated by dividing the measured OD_{600} by the initial OD_{600}.

Biofilm formation assays. Biofilm formation assays in polystyrene microtiter plates were performed as described previously (23). Briefly, strain ST1000 was cultivated overnight in TSB plus IPTG (0.05 mM). This culture was diluted to an OD_{600} of 0.1 in TSB plus 0.25% glucose with increasing concentrations of IPTG, and these dilutions were distributed in the microtiter wells (200 μl per well). After 24 h at 37°C, the wells were washed with sterile PBS, air dried, and stained with 0.1% crystal violet for 15 min. The microtiter plate was then rinsed with PBS and air dried, and the stained biomass was resuspended for quantification in ethanol-acetone (80:20). The absorbance was measured at 595 nm and normalized to the OD_{600} of each well culture (under the conditions compared in this assay, growth rates were the same).

RESULTS

WalKR-depleted cells die but do not lyse. Experiments designed to test the ability of WalKR-starved cells to recover under conditions where WalKR activity was restored showed that loss of the TCS has a bactericidal effect, with a drastic decrease in CFU following prolonged incubation after cessation of growth (13, 36). In order to evaluate the effect of a lack of WalKR on a bacterial population, we used fluorescence microscopy and the LIVE/DEAD BacLight bacterial-viability assay (Molecular Probes; see Materials and Methods) on a culture of the *S. aureus* ST1000 strain in the absence of IPTG. This strain was previously described as IPTG dependent, since the *yycFGHIJ* operon is placed under the control of the IPTG-inducible P*spac* promoter (13).

As shown in Fig. 1A, while the strain grew normally in the presence of 1 mM IPTG, growth was rapidly arrested in the absence of inducer, in agreement with the progressive dilution and loss of the WalKR proteins during the first rounds of cell division. As shown in Fig. 1B, during the exponential growth phase, the bacteria displayed green SYTO 9 fluorescence typical of healthy cells (Fig. 1B, T_1, 65 min). Immediately after

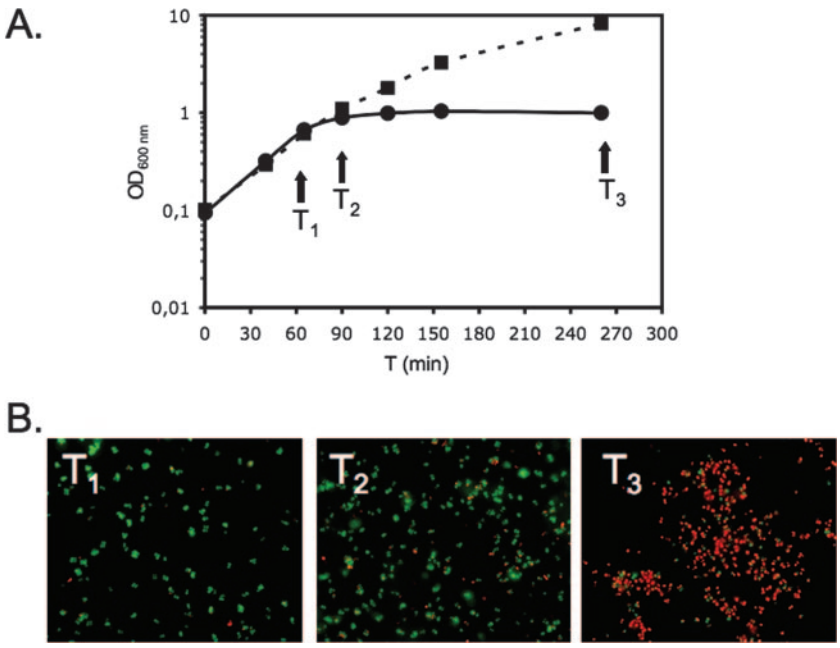

FIG. 1. Viability assay of WalKR-depleted cells. (A) IPTG-dependent growth of the conditional ST1000 mutant strain. An overnight culture in TSB plus 1 mM IPTG was diluted to an OD_{600} of 0.005 in TSB medium with (squares) or without (circles) 1 mM IPTG. At times T_1, T_2, and T_3, aliquots of the culture in TSB without IPTG were sampled for fluorescent staining. (B) Fluorescent staining of cells with the LIVE/DEAD BacLight viability kit, followed by fluorescence microscopy. SYTO 9-stained bacteria were alive and appear green, while propidium iodide-stained bacteria were dead and appear red.

cessation of growth (Fig. 1B, T_2, 90 min), more than 90% of the bacteria were viable, with less than 10% of the cells displaying red propidium iodide fluorescence characteristic of dead bacteria with damaged membranes. Approximately 3 hours after the cells stopped growing, greater than 90% of the cells were dead but maintained their structural integrity, as little or no cell lysis could be observed (Fig. 1A and B, T_3). We noted that in the absence of IPTG, cells increasingly tended to aggregate (Fig. 1B, compare T_3 to T_1). As a control for cell viability under conditions of full induction of the *walKR* operon, we stained samples of the IPTG-supplemented culture, and as expected, nearly 100% of the cells were alive at each time point tested (data not shown). These results indicate that (i) cells stop growing, not because they die, but due to some primary event that is conducive to the loss of cell viability, and (ii) although the cells die, there are no associated gross morphological changes apart from their tendency to cluster.

The WalKR TCS positively controls cell wall-hydrolytic activities. As described above, bacterial cell death due to WalKR depletion was not followed by lysis. Previous work performed in our laboratory indicated that the WalKR TCS might regulate the expression of at least one gene potentially involved in cell wall hydrolysis in *S. aureus*, *lytM* (13). The hypothesis of a link between the absence of cell lysis and an impact of the WalKR TCS on global autolysin activity in *S. aureus* was tested by examining autolytic activities of SDS-extracted proteins, using SDS-PAGE containing heat-inactivated *S. aureus* cells (zymograms). We compared lytic activities of ST1000 cells grown with or without IPTG. As shown in Fig. 1A, cells cultured without IPTG rapidly stopped growing (around an OD_{600} of 1), whereas in the presence of IPTG growth continued. Cells cultured with and without inducer were harvested immediately after cessation of growth of the WalKR-depleted strain, and SDS-extracted proteins were analyzed by zymograms following SDS-PAGE (Fig. 2) (see Materials and Methods). As shown in Fig. 2, four major hydrolytic bands of approximately 150 kDa, 100 kDa, 70 kDa, and 35 kDa could be distinguished. As previously described, this is a typical *S. aureus* autolytic profile, in which the three heavier bands correspond to the bifunctional autolysin AtlA and its processed

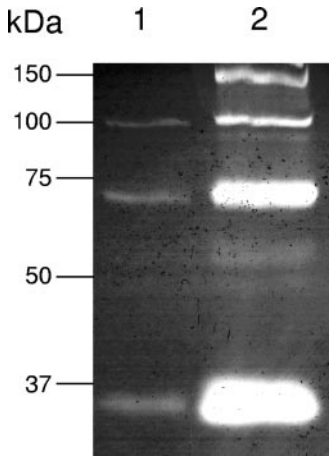

FIG. 2. Zymographic analyses of SDS-extracted proteins from strain ST1000 grown without (lane1) or with (lane 2) 1 mM IPTG. Zymographic analysis was performed following SDS-PAGE on a 10% acrylamide gel containing heat-inactivated *S. aureus* cells. The positions of molecular mass standards are indicated on the left.

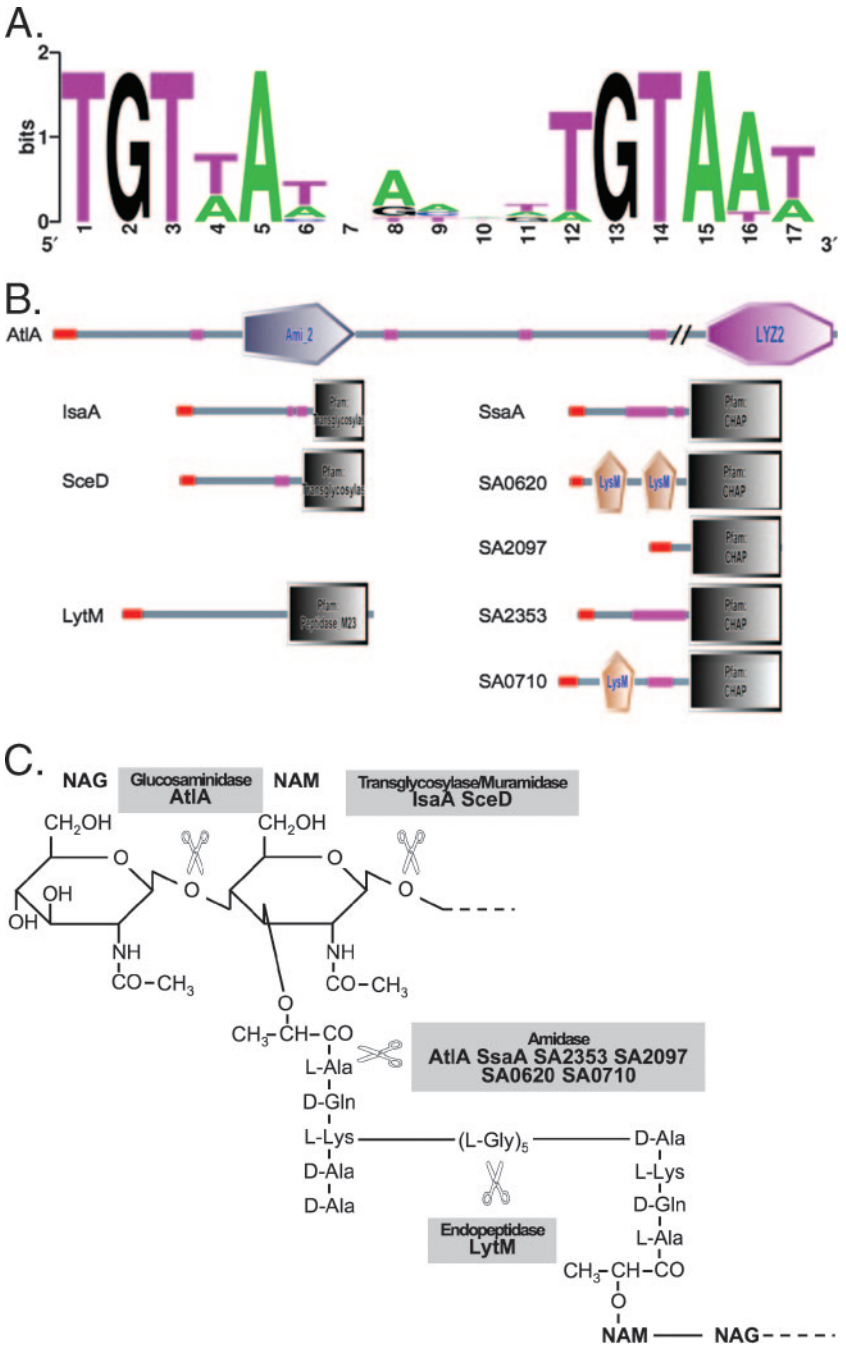

FIG. 3. Sequence logo from the putative WalR binding sites, generated using WebLogo (http://weblogo.berkeley.edu/) (8, 47). (B) Domain architecture of cell wall hydrolases encoded by putative WalKR-regulated genes based on the graphical output of the SMART web interface (http://smart.embl-heidelberg.de) (48). The red fragments represent signal peptides, and the pink sections correspond to low-complexity regions. The definitions of the boxed domains are as follows: Ami-2, *N*-acetylmuramoyl-L-alanine amidase; LYZ2, mannosyl-glycoprotein endo-β-*N*-acetylglucosamidase; LysM, peptidoglycan binding function; CHAP, cysteine, histidine-dependent aminohydrolase/peptidase; peptidase-M23, glycyl-glycine endopeptidase; transglycosylas, transglycosylase. (C) Schematic representation of *S. aureus* peptidoglycan and the known hydrolytic activities by which it is cleaved. Peptidoglycan hydrolase activities encoded by potential members of the WalKR regulon are listed.

intermediates (1, 18, 53) and the 35-kDa band corresponds to the LytM autolysin (34.4 kDa) (43). The intensities of these hydrolytic bands clearly show that when transcription of the *walKR* operon is induced, the activity levels of AtlA and LytM are strongly increased (Fig. 2), reaching a level comparable to that of the RN4220 parental strain (data not shown). This result indicates that the WalKR TCS positively controls *S. aureus* autolytic activity.

Transcriptional activation of cell wall hydrolase genes by the WalKR TCS. Our prior work on the WalKR regulons of *B. subtilis* and *S. aureus* allowed us to define a consensus binding site recognized by the WalR response regulator. This sequence

TABLE 2. Genes potentially related to cell wall degradation that have a consensus WalR binding site in their upstream regions on either the coding or the noncoding strand

Gene	Putative WalR binding site	Distance (bp) from translation start site	Strand location[a]
lytM (SA0265)	TGTAATGACAATGTAAT	158	CS
isaA (SA2356)	TGTAAAGAAAGTGTAAT	156	CS
sceD (SA1898)	TGTAATCACTGTGTAAA	129	CS
atlA (SA0905)	TGTAAATTAAGAGTATA	87	CS
ssaA (SA2093)	TGTTAACGTTTTGTAAT	136	NCS
	TGTTACAAATTTGTAAT	265	NCS
SA0620	TGTTATTATCTTGTAAT	144	NCS
SA2097	TGTTATTGATTTGTAAA	139	NCS
SA2353	TGTTATCATAATGTAAT	182	NCS
SA0710	TGTTATAACGATGTAAT	75	NCS

[a] CS, coding strand; NCS, noncoding strand.

is composed of two direct repeats separated by 5 nucleotides: 5′-TGTWAH-N5-TGTWAH-3′ (Fig. 3A) (13, 26). We identified this sequence upstream from several genes annotated as encoding proteins involved in virulence, interactions with the host matrix, oligopeptide transport, or secreted antigens (13). As shown above, WalKR controls cell wall hydrolase activity in *S. aureus*, yet apart from *lytM*, which encodes a major autolysin, none of the genes thought to be controlled by this TCS had been predicted to be involved in cell wall metabolism (13). We therefore carefully reexamined the genome annotations of genes potentially belonging to the WalKR regulon, subjecting each encoded protein to a conserved domain architecture comparison using the SMART web-based analysis tool (http://smart.embl-heidelberg.de; 34, 48). As shown in Fig. 3B and Table 2, the results of this analysis allowed new functions to be deduced for several of the predicted WalKR regulon genes, suggesting that they encode proteins with cell wall-degradative functions. Apart from the major autolysin LytM (SA0265), which has an M23 peptidase Pfam domain (16; http://www.sanger.ac.uk/Software/Pfam), SceD (SA1898) and IsaA (SA2356) share a conserved transglycosylase/muramidase domain and SsaA (SA2093) and four structurally related proteins (SA0620, SA0710, SA2097, and SA2353) all share a common CHAP amidase domain (Fig. 3B and Table 2). All of these proteins have amino-terminal signal sequences, indicating that they are likely to be exported and/or targeted to the cell wall or membrane. A schematic representation of *S. aureus* peptidoglycan and the known hydrolytic activities is shown in Fig. 3C, indicating that potential members of the WalKR regulon encode enzymes corresponding to all the different types of peptidoglycan degradation activities, i.e., glucosaminidase, transglycosylase/muramidase, amidase, and endopeptidase (Fig. 3C).

The region upstream from the *atlA* (SA0905) gene also contains a potential WalR binding site (Table 2), albeit with two mismatches (boldface italics) (TGTAAA-N5-*A*GTA*T*A instead of 5′-TGTWAH-N5-TGTWAH-3′), located 54 bp upstream from the previously determined transcription start site (42). We had previously shown that purified WalR could bind in vitro upstream from the *lytM*, *isaA*, and *ssaA* genes, but it remained to be determined whether WalKR in fact controlled the expression of genes preceded by proven or potential WalR binding sites. We therefore examined the effect of induction of *walKR* expression on the transcription of these genes. cDNA was synthesized from equal amounts of total RNA from exponential-phase cultures (OD_{600}, ~1.2) of strain ST1000 grown in the presence of 0.05 mM or 1 mM IPTG (low and high levels of WalKR, respectively). Relative amounts of specific cDNA corresponding to the transcripts of *lytM*, *sceD*, *isaA*, *atlA*, and *ssaA* and its four related genes (SA2353, SA2097, SA0620, and SA0710) were measured by qRT-PCR using specific oligonucleotide pairs (Table 1) (see Materials and Methods).

As shown in Fig. 4, the *walKR* induction factor with low or high IPTG concentrations was reproducibly around sixfold, indicating that these conditions allow significant variation in *walKR* expression levels. Our results show that the mRNA levels of all nine genes increased, along with *walKR* transcription. The induction rates for expression of these genes varied from about 2-fold to more than 14-fold, suggesting that transcriptional activation by the WalKR TCS is not the same at each promoter. This could be due to the positioning of the WalR binding site relative to the promoter region, as well as variations in the consensus promoter sequences. These results were confirmed by primer extension experiments performed with the *lytM* transcript showing that expression levels closely follow those of *walKR* within the cell (Fig. 5A). The nucleotide sequence of the region preceding the *lytM* transcription start site revealed appropriately spaced potential −10 and −35 regions sharing similarities with the consensus sequence of promoters recognized by the vegetative form of RNA polymerase, $E\sigma^A$ (Fig. 5B). The previously established DNase I footprint of bound WalR extends from positions −80 to −117 with respect to the *lytM* transcription start site and is located 43 base pairs upstream from the −35 sequence, in agreement with the role of WalR as a positive regulator of transcription.

WalKR-depleted cells display increased aggregation. We have shown that the WalKR TCS has a positive effect on major autolytic activities of *S. aureus*. These activities are involved in many crucial cell functions and influence *S. aureus* development. One of the well-characterized phenotypes of several mutants in genes encoding cell wall hydrolases is their tendency to aggregate, since autolysins are involved in daughter cell separation (particularly AtlA), but also because cell-to-cell adherence is higher (3, 52, 56). As shown in Fig. 6A, cell clusters were apparent in a static liquid culture of strain ST1000 cultivated in TSB without IPTG whereas in the presence of inducer the cells were well separated (Fig. 6B). Fields for the cultures grown without inducer showed large numbers of clusters, and a representative field is shown. By contrast, when cultures were grown with shaking, the clusters were much less apparent and the fields for the ST1000 strain with or without inducer were similar (data not shown). This cell aggregation phenotype suggests that the WalKR system affects cell organization, favoring a compact population structure instead of cellular dissemination.

WalKR-starved cells are resistant to Triton X-100-induced lysis. To verify whether the positive effect of WalKR levels on hydrolytic activities is associated with increased susceptibility to cell lysis, we tested the effect of a nonionic detergent, Triton X-100, on autolysis. Triton X-100 is thought to trigger autolysis by removing lipoteichoic acids, which act as inhibitors of en-

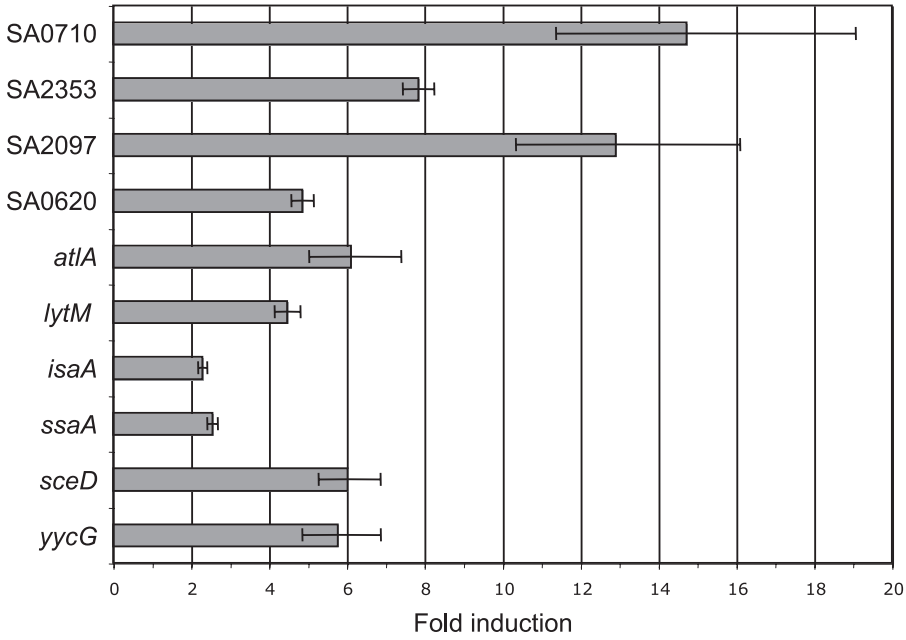

FIG. 4. Effect of *walKR* induction on transcription of genes involved in cell wall degradation. Total RNA was extracted from ST1000 cells grown in TSB supplemented with 0.05 mM or 1 mM IPTG. After reverse transcription, specific cDNAs were quantified by qRT-PCR. The results are expressed as the means and standard deviations of quadruplicate experiments using primers specific for target genes and 16S rRNA (normalizing gene).

dogenous autolysins (44). Strain ST1000 was grown in TSB without inducer or with 0.05 mM or 1 mM IPTG to an OD_{600} of ~1 (the growth rates of the cultures were identical until that point). Cells were then harvested and resuspended in PBS (control) or PBS containing 0.1% Triton X-100 (see Materials and Methods).

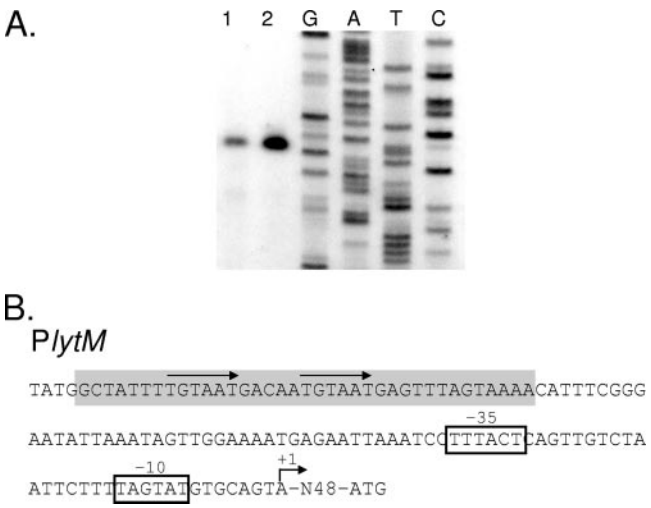

FIG. 5. Primer extension analysis of the *lytM* transcript. (A) Total RNA was extracted from cultures of strain ST1000 grown in TSB supplemented with 0.05 mM IPTG (lane 1) or 1 mM IPTG (lane 2) to an OD_{600} of 1.2. Primer extensions were performed using a *lytM*-specific primer (OSA91). Sanger sequencing reactions (GATC) were carried out on a PCR fragment (OSA90-OSA91) corresponding to the *lytM* upstream region. (B) Nucleotide sequence of the *lytM* upstream region. The ATG codon is indicated. The transcription start site is labeled +1, and the consensus −10 and −35 sequences are boxed. The extent of the previously characterized WalR DNase I footprint is shaded, and the WalR binding site is indicated by arrows.

As shown in Fig. 7A, the WalKR-depleted culture exhibited high resistance to Triton X-100-induced autolysis, since less than 5% lysis was observed after 3 h. Comparisons of results obtained with the low- and high-induction cultures (induction with 0.05 mM IPTG and 1 mM IPTG, respectively) confirmed this result, since the resistance of the low-induction culture was intermediate (50% lysis was observed after 3 h for the low-induction culture versus 2 h for the high-induction culture) (Fig. 7A). Lysis in the control experiment, in which cells were resuspended in PBS without Triton X-100, was less than 5% over the same period for the three culture conditions tested (data not shown).

WalKR depletion leads to increased resistance to lysostaphin-induced lysis. As shown above, autolytic activities of *S. aureus* are up-regulated by the WalKR TCS. To determine whether this regulation entails modifications of cell wall structure, we examined the effect of WalKR depletion on lysostaphin sensitivity. Lysostaphin is a glycyl-glycine endopeptidase that specifically cleaves the pentaglycine cross-bridges of the staphylococcal cell wall, leading to rapid lysis of the bacteria.

Strain ST1000 was grown in TSB or TSB plus 1 mM IPTG to an OD_{600} of ~1, and the cells were resuspended in PBS. Lysostaphin lysis tests were then carried out on the nongrowing cells. As shown in Fig. 7B, our experimental conditions (incubation in PBS in the presence of 200 ng/ml lysostaphin at 37°C) led to 50% cell lysis in 10 min, and 90% of the cells were lysed by the end of the assay, when *walKR* expression was fully induced. In contrast, cells uninduced for *walKR* expression displayed a lower lysis rate, and less than 40% of the cells were

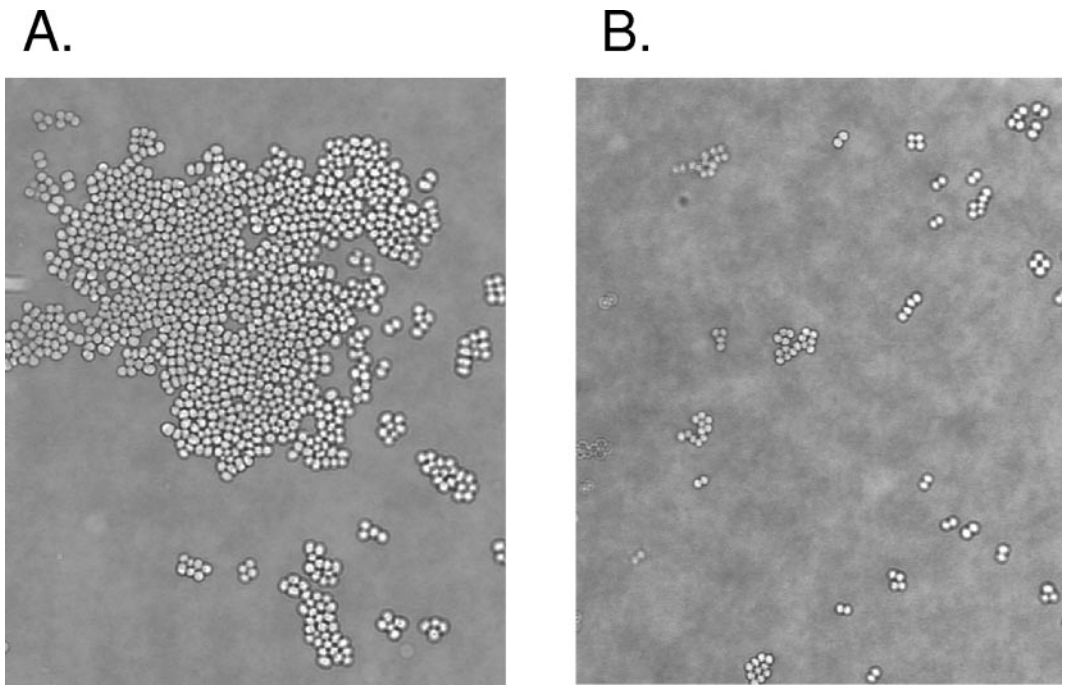

FIG. 6. Phase-contrast micrographs (magnification, ×1,000) of strain ST1000 cultivated in TSB medium without (A) or with (B) 1 mM IPTG. Fields for the cultures grown without inducer showed large numbers of clusters; a representative field is shown.

lysed at the end of the assay. These data show that depletion of WalKR leads to increased lysostaphin resistance. This effect could be due to a modification of peptidoglycan conformation or composition resulting in lowered accessibility of the penta-glycine bonds targeted by lysostaphin or a synergistic effect of lysostaphin with WalKR-activated autolysins.

WalKR depletion modifies cell wall composition. Since WalKR depletion resulted in several changes in cell wall prop-

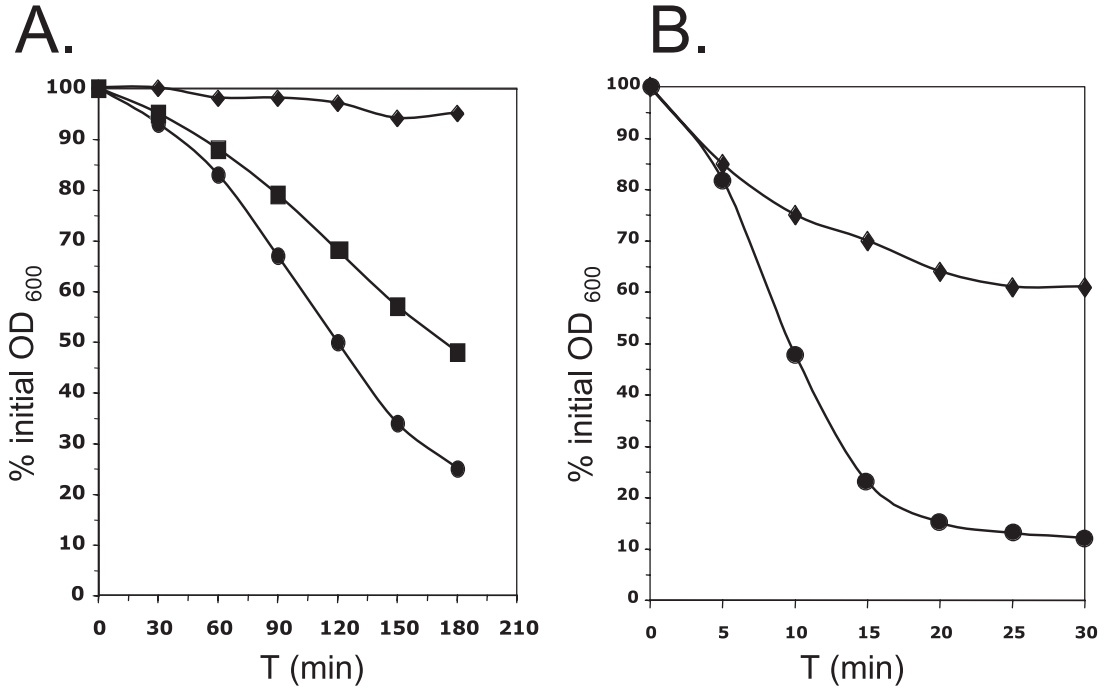

FIG. 7. Autolysis profiles upon *walKR* induction. Strain ST1000 was grown in TSB without IPTG (◆) or with 0.05 mM IPTG (■), or 1 mM IPTG (●) to an OD_{600} of 1. The cells were then pelleted and resuspended in PBS to test the effects of autolysis-inducing agents. Triton- and lysostaphin-mediated lysis of staphylococci was measured as the decline of OD_{600} over time. (A) Autolysis determined at 30°C in the presence of 0.1% Triton X-100. (B) Autolysis determined at 37°C in the presence of 200 ng/ml lysostaphin.

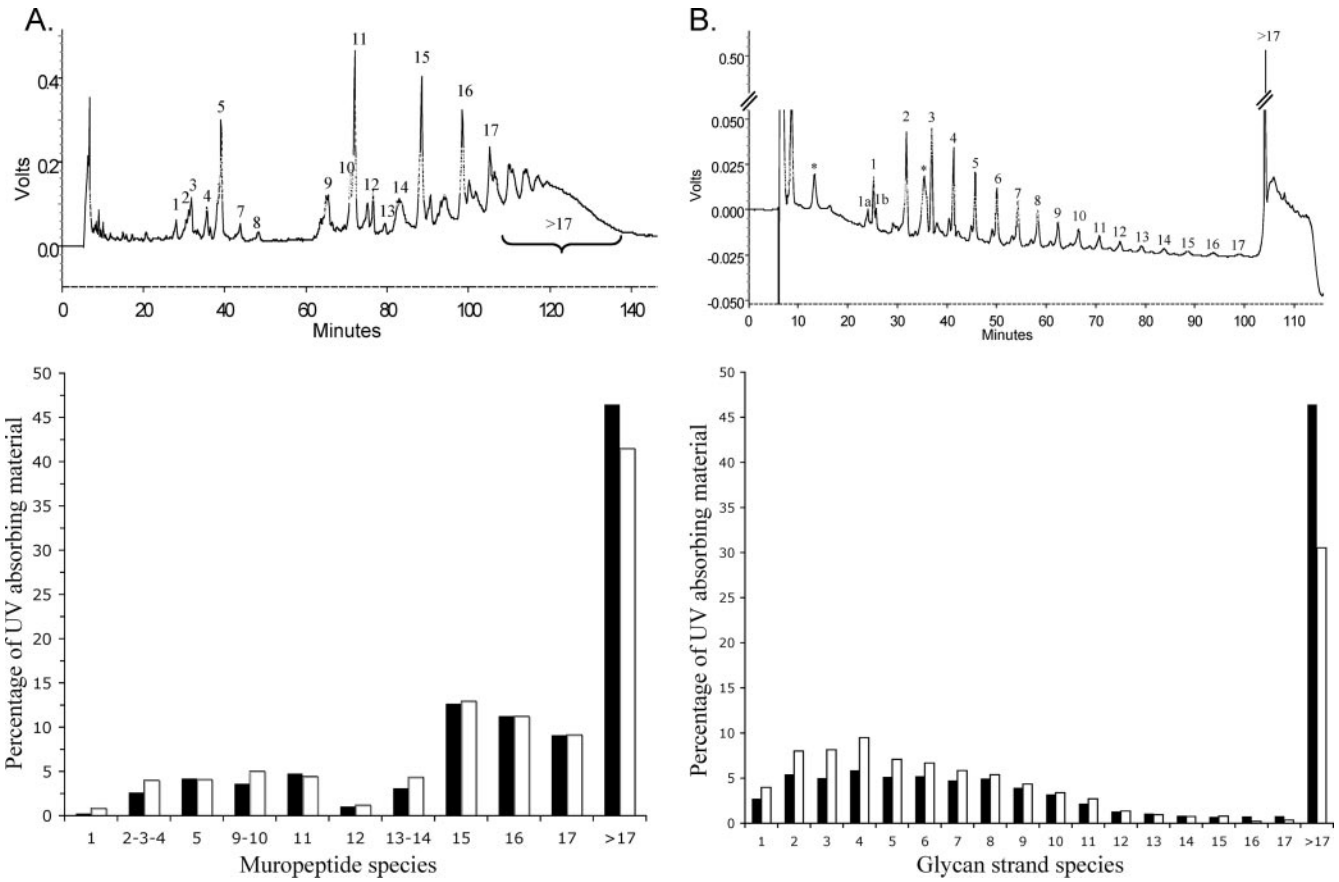

FIG. 8. Effect of WalKR depletion on *S. aureus* peptidoglycan structure. Structural analysis was performed by determining the muropeptide composition (A) and glycan strand length distribution (B). ST1000 cells were grown with (white bars) or without (black bars) 1 mM IPTG and harvested immediately after the cessation of growth in the absence of inducer. (A) Muropeptide nomenclature was as previously described. The upper graph represents the HPLC muropeptide elution profile of the ST1000 strain grown with 1 mM IPTG and the identification of the muropeptide species (10). Briefly, muropeptides 1 to 7 correspond to monomeric muropeptides, 11 to 14 to dimeric muropeptides, 15 to trimers, 16 to tetramers, and 17 to pentamers. Highly oligomeric muropeptides elute as an unresolved "hump." (B) Glycan strand species nomenclature corresponds to the number of disaccharide *N*-acetylglucosamine-β(1, 4)-*N*-acetylmuramic acid repeating units (5). The HPLC elution profile and identification of glycan strand species are shown in the upper graph. Satellite peaks were observed in low abundance and were excluded to simplify the analysis, since they did not change under the conditions tested (data not shown).

erties and synthesis of both endopeptidases (LytM) and hexosaminidases (IsaA, SceD, and AtlA), we decided to perform peptidoglycan structural analysis in the presence or absence of the TCS. Peptidoglycan was purified from ST1000 cells grown with or without 1 mM IPTG just after growth arrest of the WalKR-depleted strain. Purified peptidoglycan was digested either with the muramidase mutanolysin or with the recombinant amidase domain of the AtlA protein. Using high-pressure liquid chromatography (HPLC), we compared muropeptide compositions and glycan strand length distributions for the two growth conditions. WalKR depletion resulted in a modest increase in cross-linking (oligomeric material increased from 41.5% to 46.5%) and a decrease in muropeptides 2, 3, 4, 9, 10, and 14 (Fig. 8A), structures that are consistent with glycylglycine endopeptidase degradation products (10).

Interestingly, muropeptide 1, i.e., *N*-acetylglucosamine-β(1,4)-*N*-acetylmuramic acid pentapeptide levels were lowered approximately fourfold, becoming virtually absent following WalKR depletion, likely reflecting a complete arrest of de novo peptidoglycan synthesis, as well as turnover (Fig. 8A). WalKR depletion had a more pronounced effect on the glycan strand length distribution, with an increase in the numbers of very long glycans (>17 disaccharide repeating units) and a decrease in short glycan species (Fig. 8B). As previously observed for strains COL and 27s (5), strain ST1000 produced satellite peaks corresponding to glucosaminidase activity, but their proportions did not vary under the two growth conditions (data not shown). The observed increase in very long glycans could be due to WalKR-dependent control of the potential muramidase activities of IsaA and SceD, since AtlA was previously shown not to play a role in glycan strand maturation (5).

WalKR has a positive effect on both peptidoglycan biosynthesis and turnover. As suggested by determination of cell wall composition, the WalKR system has an effect not only on cell wall degradation, but also on peptidoglycan biosynthesis. In order to measure the global impact of WalKR on cell wall turnover, we compared the rates of biosynthesis and turnover of peptidoglycan in the ST1000 strain grown with and without 1 mM IPTG. Peptidoglycan

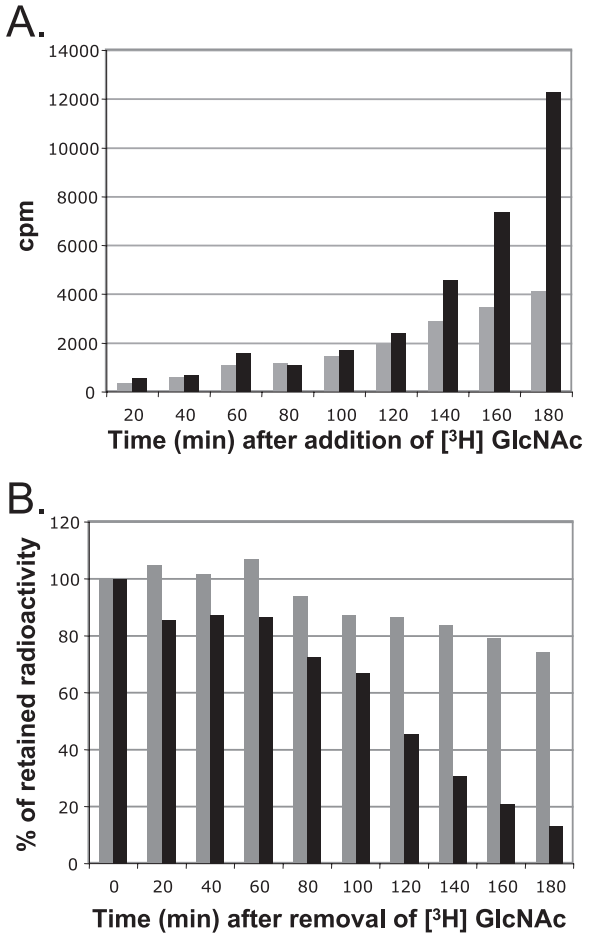

FIG. 9. Effect of WalKR depletion on cell wall biosynthesis and turnover. (A) Cell wall biosynthesis of strain ST1000 grown with (black bars) and without (gray bars) 1 mM IPTG. Cell wall biosynthesis was measured as the incorporation of [^{3}H]GlcNAc over time. (B) Cell wall turnover of strain ST1000 grown with (black bars) or without (gray bars) IPTG. Turnover was measured following [^{3}H]GlcNAc labeling as the decrease of incorporated radioactivity over time. The results are expressed as the percentage of the initial quantity of cell-associated radioactivity.

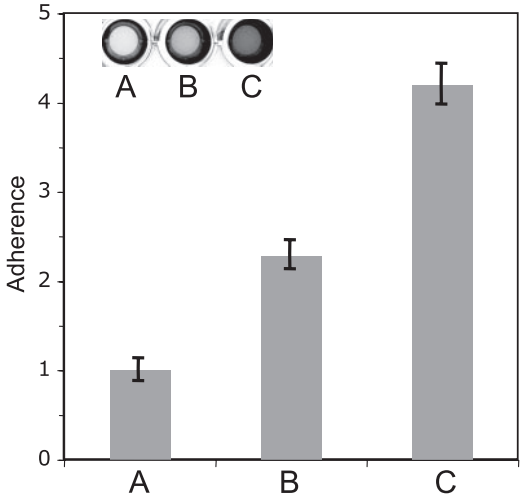

FIG. 10. Biofilm formation of strain ST1000 in the presence of increasing concentrations of IPTG. Biofilm assays were performed on microtiter plates in TSB plus 0.25% glucose with increasing concentrations of IPTG: 0.05 mM (A), 0.5 mM (B), and 1 mM (C). Quantifications were performed by measuring the OD_{595} following crystal violet staining and resuspension in ethanol-acetone (80:20). All cultures had the same growth rate, and the data were normalized to the OD_{600} of each cell culture and presented as variation (*n*-fold) compared to condition A. The results represent the mean values ± standard deviations of duplicate quantifications. Similar results were obtained in three independent experiments.

biosynthesis was measured by incorporation of [^{3}H]GlcNAc (see Materials and Methods).

As shown in Fig. 9A, when expression of the *walKR* operon was induced by 1 mM IPTG, labeling increased exponentially, indicating progressive incorporation of [^{3}H]GlcNAc following cell division. In contrast, when the expression of the *walKR* operon was shut off, incorporation of [^{3}H]GlcNAc was markedly reduced, reaching only 33% of that of the culture in the presence of WalKR over the assay period, and appeared to be linear, indicating impaired peptidoglycan biosynthesis. This result confirmed our conclusion (see above) that the decrease in muropeptide 1 levels under conditions of WalKR depletion was indeed due to reduced de novo peptidoglycan synthesis. Growth of the strain was verified under the conditions used for the assay, and the growth rates were similar in the presence and absence of IPTG, except for the last time point (180 min after the beginning of labeling), corresponding to cessation of growth in the absence of inducer (data not shown).

The global effect of WalKR on cell wall turnover was measured as the decrease in cell-bound [^{3}H]GlcNAc over time during growth in the presence of an excess of unlabeled GlcNAc (see Materials and Methods). Figure 9B shows that cell wall turnover was clearly slower when the *walKR* operon was not induced, with a measured turnover of only 26% at the end of the assay (corresponding to the decrease in cell wall-incorporated [^{3}H]GlcNAc over about six generations), whereas when the *walKR* operon was induced, cell wall turnover reached 87%. Growth of the strain was checked under the conditions used for the assay, and the growth rates were similar in the presence or absence of IPTG, except for the last two time points (160 min and 180 min after the beginning of labeling), corresponding to cessation of growth in the absence of inducer (data not shown).

WalKR positively controls biofilm formation. The ability to form biofilms is one of the main causes of the high prevalence of *S. aureus* nosocomial infections. In several cases, autolytic activity, such as that of AtlA, has been linked to biofilm formation (3, 24, 29). Since WalKR controls *S. aureus* autolytic activities, including AtlA synthesis, the effect of the TCS on biofilm formation was tested. Strain ST1000 was grown for 24 h in TSB with increasing concentrations of IPTG, and cells loosely bound to the surface (in polystyrene microtiter plates) were removed by rinsing the plates with PBS. There was a clear increase in bound biomass as IPTG levels were increased, and cells adhering to the surfaces were stained with crystal violet and quantified by measuring the OD_{595}. Cultures had the same growth rate, as measured by following the OD_{600}. As shown in Fig. 10, biofilm formation was directly dependent on IPTG concentrations, i.e., on

WalKR levels in the cell (Fig. 10A to C), indicating that the TCS positively controls *S. aureus* biofilm formation.

DISCUSSION

The data reported in this paper are the first to show a direct link between cell wall remodeling and the WalKR TCS. We have shown that WalKR activates the transcription of nine genes involved in all the different steps of cell wall degradation (*lytM*, *atlA*, *isaA*, *sceD*, *ssaA*, and four *ssaA*-related genes), all of which are preceded by potential WalR binding sites. In a previous report, we showed direct binding of the WalR regulator to the promoter regions of *lytM*, *isaA*, and *ssaA* (13). Taken together, these results suggest that WalR binds to the upstream regions of these nine genes and enhances transcription from their promoters. Autolytic activities of *S. aureus* were also positively controlled by WalKR, including those of the two major autolysins, AtlA and LytM, and the lysis rate of *S. aureus* in the presence of Triton X-100 was enhanced by the WalKR system. Furthermore, enhanced resistance to lysostaphin was observed in cells starved for WalKR, suggesting a more global effect of this system on cell wall composition.

Peptidoglycan composition analyses indicated that WalKR depletion led to increases in peptidoglycan cross-linking and glycan chain length, modifications that correlate with the demonstrated regulation of cell wall hydrolases. In addition, we observed the disappearance of *N*-acetylglucosamine-β(1,4)-*N*-acetylmuramic acid pentapeptide in the absence of WalKR, indicating a likely arrest of cell wall synthesis. Indeed, cell wall biosynthesis was strongly decreased when the WalKR system was absent. We have also shown that WalKR is required for cell wall turnover, probably due to its positive role in controlling both peptidoglycan biosynthesis and degradation. We have yet to identify WalKR-regulated genes directly involved in cell wall biosynthesis, which could suggest that this effect might be indirectly due to an arrest in cell wall degradation, but we cannot exclude the possibility that our proposed consensus binding site was too restrictive to allow us to identify the entire WalKR regulon. Indeed, *atlA* transcription is activated by WalKR, although its upstream region contains a degenerate WalKR binding site.

Cell wall integrity is critical for viability, and cell wall metabolism genes are known to be tightly regulated. Three regulatory systems have been shown to repress cell wall-hydrolytic activities in *S. aureus*, the LytSR and ArlSR TCSs and the Rat regulator (6, 19, 27). WalKR is the first TCS identified as positively controlling cell wall hydrolase synthesis. Previous work on the WalKR regulon, especially in *B. subtilis* and *S. pneumoniae*, suggested a role for the TCS in cell wall metabolism. In *B. subtilis*, we showed specific interactions between WalR and the promoter regions of four genes involved in cell wall metabolism. These genes encode YocH and YkvT, two potential cell wall hydrolases, as well as the teichoic acid biosynthesis enzymes TagA/TagD (26).

In *S. pneumoniae*, genome-wide expression profiling under conditions of depletion of VicKR (the *S. pneumoniae* WalKR orthologue) showed a decrease in transcription for two genes involved in cell wall degradation, spr0867 and spr2021 (37, 40). The first encodes a protein with several cell wall binding domains and a domain with endo-β-*N*-acetylglucosaminidase activity and has been characterized as the LytB murein hydrolase (12). The spr2021 gene encodes PcsB, a protein with an amidase domain that has been linked to cell separation during cellular division (45). The VicK kinase (a WalK orthologue) is not essential in streptococcal species, and it has been shown that the essential VicR regulator (a WalR orthologue) is not required in *S. pneumoniae* when the *pcsB* gene is constitutively expressed (40). It is interesting that the *S. mutans* PcsB homolog, GbpB, is also regulated by the VicKR (WalKR) system, while it has not been elucidated whether this is correlated with the essentiality of the *vicR* (*walR*) gene (49).

In a previous study, we identified 31 genes potentially regulated by the WalKR TCS in *S. aureus* and showed specific binding of WalR to the promoter regions of three of them (*ssaA*, *isaA*, and *lytM*) (13). We show here that the presence of WalR binding sites is associated with transcription activation for nine genes involved with cell wall metabolism, defining the major function of the *S. aureus* WalKR regulon.

The WalKR (originally YycGF) TCS has been referred to by several names in different bacteria, such as MicBA for its reported role in controlling competence in *S. pneumoniae* and VicKR in *S. pneumoniae* and *S. mutans* for its role in virulence and competence (14, 54). Considering that WalKR is very highly conserved among low-G+C gram-positive bacteria and that several of these are neither naturally competent (*S. aureus* and *L. monocytogenes*) nor pathogenic (*B. subtilis*), we believe this diverse nomenclature is confusing and inappropriate. Given the plethora of data now firmly establishing the major role of WalKR in cell wall metabolism in all the bacteria in which it has been studied and in an effort both to simplify the nomenclature and to refer to this TCS by a name which truly reflects its function, we propose referring to it henceforth as WalK (YycG histidine kinase) and WalR (YycF response regulator).

Among the predicted WalKR-regulated genes, none have been found to be essential in *S. aureus* by genome-wide screening using antisense RNA (17, 28). Nevertheless, our data show a global regulation of cell wall hydrolases by the WalKR system. Cell wall hydrolases have been shown to be involved in numerous cellular processes crucial for cell physiology, such as peptidoglycan maturation, cell wall turnover, cell separation, and protein secretion (50). Genes encoding cell wall hydrolases are highly redundant in bacterial genomes. In *S. pneumoniae*, two genes encode CHAP domain proteins with an amidase activity: *pcsB*, an essential gene whose activation is responsible for WalR essentiality, and *cbpD*, encoding a choline binding protein involved in competence-induced cell lysis (31). In *S. aureus*, however, there are more than 10 genes encoding putative amidases with a CHAP domain (based on data from the SMART database), and we have shown that WalKR regulates at least 5 of them. This strongly suggests that the essential nature of WalKR in *S. aureus* is probably not linked to the regulation of a single gene but is likely to be multifactorial, involving global regulation of redundant cell wall-related functions. Studies are now in progress to test this hypothesis.

Cell wall metabolism is involved in many cellular processes; thus, as expected, modifications of peptidoglycan degradation are linked to a wide range of phenotypes. The first characteristic associated with modulation of cell wall hydrolases is sensitivity to compounds that target the cell wall, particularly

antibiotics. A second well-documented phenotype associated with a defect in autolysins is the propensity of planktonic cell suspensions to aggregate. This has been particularly well studied with AtlA, since cells of an *atlA* mutant strain aggregate in liquid culture and this phenotype can be reversed by the addition of purified AtlA to the cell suspension (52, 53). A similar phenotype is associated with the absence of a more recently identified amidase-type autolysin, Sle-1 (29). The aggregation/cell separation defect phenotype of AtlA- or Sle-1-deficient strains has been at least partly correlated with the role of these autolysins in the splitting of the septum during cell division, whereas a possible effect on noncovalent cell-to-cell adherence remains to be specifically characterized (1, 29, 56).

A more unexpected function of autolysins is their involvement in biofilm formation. While autolysin-deficient strains show increased intercellular interactions (formation of clusters), they are impaired in their capacity to form biofilms because of a defect in primary attachment, as shown for *atlA* and *atlE* mutants of *S. aureus* and *Staphylococcus epidermidis*, respectively (3, 24). In agreement with our results on the activation of autolytic activities by the WalKR system, we have shown that depletion of this system leads to phenotypes directly related to a lack of autolysins, e.g., higher resistance to cell wall-active compounds (Triton X-100 and lysostaphin), cell aggregation, and impaired biofilm formation. In *S. mutans*, WalKR has also been shown to positively control biofilm formation (49). Interconnections with cell wall-hydrolytic activities were not studied in *S. mutans*, but several phenotypes resulting from disruption of *walK*, encoding the kinase, suggest that it could be involved in controlling autolysin activities (cell clustering and rough cell surface) (49).

Peptidoglycan dynamics play a central role in bacterial pathogenesis, because of its role in maintaining cell shape and in exposing cell wall-anchored proteins, but also because peptidoglycan degradation products, muropeptides, are powerful virulence effectors (4). Many covalently cell wall-anchored polymers, such as teichoic acid or sortase-dependent proteins, have been shown to play a role in *S. aureus* virulence, and thus, it is likely that any factor interfering with cell wall turnover, as shown here for the WalKR system, could influence the exposure of virulence determinants at the bacterial surface. Moreover, it has been shown that released muropeptides (cell wall degradation products) play a major role in induction of the proinflammatory response (21). As the WalKR system controls the expression of genes encoding cell wall hydrolases, it could influence the proinflammatory response and consequently the capacity of the host organism to combat *S. aureus* in the early stages of infection. Future research will aim at characterizing the impact of WalKR-dependent control of *S. aureus* virulence.

ACKNOWLEDGMENTS

This work was supported by research funds from the European Commission (grants from BACELL Health [LSHG-CT-2004-503468], StaphDynamics [LHSM-CT-2006-019064], and BaSysBio [LSHG-CT-2006-037469]), the Centre National de la Recherche Scientifique (CNRS URA 2172), and the Institut Pasteur (Grand Programme Horizontal no. 9). I. G. Boneca is an INSERM research scientist.

We thank Georges Rapoport for critical reading of the manuscript, as well as Ivica Letunic for kind assistance with the SMART web interface graphical output.

REFERENCES

1. **Baba, T., and O. Schneewind.** 1998. Targeting of muralytic enzymes to the cell division site of Gram-positive bacteria: repeat domains direct autolysin to the equatorial surface ring of *Staphylococcus aureus*. EMBO J. **17:**4639–4646.
2. **Benton, B. M., J. P. Zhang, S. Bond, C. Pope, T. Christian, L. Lee, K. M. Winterberg, M. B. Schmid, and J. M. Buysse.** 2004. Large-scale identification of genes required for full virulence of *Staphylococcus aureus*. J. Bacteriol. **186:**8478–8489.
3. **Biswas, R., L. Voggu, U. K. Simon, P. Hentschel, G. Thumm, and F. Gotz.** 2006. Activity of the major staphylococcal autolysin Atl. FEMS Microbiol. Lett. **259:**260–268.
4. **Boneca, I. G.** 2005. The role of peptidoglycan in pathogenesis. Curr. Opin. Microbiol. **8:**46–53.
5. **Boneca, I. G., Z. H. Huang, D. A. Gage, and A. Tomasz.** 2000. Characterization of *Staphylococcus aureus* cell wall glycan strands, evidence for a new beta-*N*-acetylglucosaminidase activity. J. Biol. Chem. **275:**9910–9918.
6. **Brunskill, E. W., and K. W. Bayles.** 1996. Identification of LytSR-regulated genes from *Staphylococcus aureus*. J. Bacteriol. **178:**5810–5812.
7. **Chastanet, A., M. Prudhomme, J. P. Claverys, and T. Msadek.** 2001. Regulation of *Streptococcus pneumoniae clp* genes and their role in competence development and stress survival. J. Bacteriol. **183:**7295–7307.
8. **Crooks, G. E., G. Hon, J. M. Chandonia, and S. E. Brenner.** 2004. WebLogo: a sequence logo generator. Genome Res. **14:**1188–1190.
9. **Day, N. P., C. E. Moore, M. C. Enright, A. R. Berendt, J. M. Smith, M. F. Murphy, S. J. Peacock, B. G. Spratt, and E. J. Feil.** 2001. A link between virulence and ecological abundance in natural populations of *Staphylococcus aureus*. Science **292:**114–116.
10. **de Jonge, B. L., Y. S. Chang, D. Gage, and A. Tomasz.** 1992. Peptidoglycan composition of a highly methicillin-resistant *Staphylococcus aureus* strain. The role of penicillin binding protein 2A. J. Biol. Chem. **267:**11248–11254.
11. **de Jonge, B. L., H. de Lencastre, and A. Tomasz.** 1991. Suppression of autolysis and cell wall turnover in heterogeneous Tn*551* mutants of a methicillin-resistant *Staphylococcus aureus* strain. J. Bacteriol. **173:**1105–1110.
12. **De Las Rivas, B., J. L. Garcia, R. Lopez, and P. Garcia.** 2002. Purification and polar localization of pneumococcal LytB, a putative endo-beta-*N*-acetylglucosaminidase: the chain-dispersing murein hydrolase. J. Bacteriol. **184:**4988–5000.
13. **Dubrac, S., and T. Msadek.** 2004. Identification of genes controlled by the essential YycG/YycF two-component system of *Staphylococcus aureus*. J. Bacteriol. **186:**1175–1181.
14. **Echenique, J. R., and M. C. Trombe.** 2001. Competence repression under oxygen limitation through the two-component MicAB signal-transducing system in *Streptococcus pneumoniae* and involvement of the PAS domain of MicB. J. Bacteriol. **183:**4599–4608.
15. **Fabret, C., and J. A. Hoch.** 1998. A two-component signal transduction system essential for growth of *Bacillus subtilis*: implications for anti-infective therapy. J. Bacteriol. **180:**6375–6383.
16. **Finn, R. D., J. Mistry, B. Schuster-Bockler, S. Griffiths-Jones, V. Hollich, T. Lassmann, S. Moxon, M. Marshall, A. Khanna, R. Durbin, S. R. Eddy, E. L. Sonnhammer, and A. Bateman.** 2006. Pfam: clans, web tools and services. Nucleic Acids Res. **34:**D247–D251.
17. **Forsyth, R. A., R. J. Haselbeck, K. L. Ohlsen, R. T. Yamamoto, H. Xu, J. D. Trawick, D. Wall, L. Wang, V. Brown-Driver, J. M. Froelich, G. C. Kedar, P. King, M. McCarthy, C. Malone, B. Misiner, D. Robbins, Z. Tan, Z. Y. Zhu Zy, G. Carr, D. A. Mosca, C. Zamudio, J. G. Foulkes, and J. W. Zyskind.** 2002. A genome-wide strategy for the identification of essential genes in *Staphylococcus aureus*. Mol. Microbiol. **43:**1387–1400.
18. **Foster, S. J.** 1995. Molecular characterization and functional analysis of the major autolysin of *Staphylococcus aureus* 8325/4. J. Bacteriol. **177:**5723–5725.
19. **Fournier, B., and D. C. Hooper.** 2000. A new two-component regulatory system involved in adhesion, autolysis, and extracellular proteolytic activity of *Staphylococcus aureus*. J. Bacteriol. **182:**3955–3964.
20. **Fukuchi, K., Y. Kasahara, K. Asai, K. Kobayashi, S. Moriya, and N. Ogasawara.** 2000. The essential two-component regulatory system encoded by *yycF* and *yycG* modulates expression of the *ftsAZ* operon in *Bacillus subtilis*. Microbiology **146:**1573–1583.
21. **Girardin, S. E., I. G. Boneca, J. Viala, M. Chamaillard, A. Labigne, G. Thomas, D. J. Philpott, and P. J. Sansonetti.** 2003. Nod2 is a general sensor of peptidoglycan through muramyl dipeptide (MDP) detection. J. Biol. Chem. **278:**8869–8872.
22. **Hancock, L. E., and M. Perego.** 2004. Systematic inactivation and phenotypic characterization of two-component signal transduction systems of *Enterococcus faecalis* V583. J. Bacteriol. **186:**7951–7958.
23. **Heilmann, C., C. Gerke, F. Perdreau-Remington, and F. Gotz.** 1996. Characterization of Tn*917* insertion mutants of *Staphylococcus epidermidis* affected in biofilm formation. Infect. Immun. **64:**277–282.
24. **Heilmann, C., M. Hussain, G. Peters, and F. Gotz.** 1997. Evidence for autolysin-mediated primary attachment of *Staphylococcus epidermidis* to a polystyrene surface. Mol. Microbiol. **24:**1013–1024.

25. **Henner, D. J.** 1990. Inducible expression of regulatory genes in *Bacillus subtilis*. Methods Enzymol. **185:**223–228.
26. **Howell, A., S. Dubrac, K. K. Andersen, D. Noone, J. Fert, T. Msadek, and K. Devine.** 2003. Genes controlled by the essential YycG/YycF two-component system of *Bacillus subtilis* revealed through a novel hybrid regulator approach. Mol. Microbiol. **49:**1639–1655.
27. **Ingavale, S. S., W. Van Wamel, and A. L. Cheung.** 2003. Characterization of RAT, an autolysis regulator in *Staphylococcus aureus*. Mol. Microbiol. **48:** 1451–1466.
28. **Ji, Y., B. Zhang, S. F. Van Horn, P. Warren, G. Woodnutt, M. K. Burnham, and M. Rosenberg.** 2001. Identification of critical staphylococcal genes using conditional phenotypes generated by antisense RNA. Science **293:**2266–2269.
29. **Kajimura, J., T. Fujiwara, S. Yamada, Y. Suzawa, T. Nishida, Y. Oyamada, I. Hayashi, J. Yamagishi, H. Komatsuzawa, and M. Sugai.** 2005. Identification and molecular characterization of an *N*-acetylmuramyl-L-alanine amidase Sle1 involved in cell separation of *Staphylococcus aureus*. Mol. Microbiol. **58:**1087–1101.
30. **Kallipolitis, B. H., and H. Ingmer.** 2001. *Listeria monocytogenes* response regulators important for stress tolerance and pathogenesis. FEMS Microbiol. Lett. **204:**111–115.
31. **Kausmally, L., O. Johnsborg, M. Lunde, E. Knutsen, and L. S. Havarstein.** 2005. Choline-binding protein D (CbpD) in *Streptococcus pneumoniae* is essential for competence-induced cell lysis. J. Bacteriol. **187:**4338–4345.
32. **Kuroda, M., H. Kuroda, T. Oshima, F. Takeuchi, H. Mori, and K. Hiramatsu.** 2003. Two-component system VraSR positively modulates the regulation of cell-wall biosynthesis pathway in *Staphylococcus aureus*. Mol. Microbiol. **49:**807–821.
33. **Lange, R., C. Wagner, A. de Saizieu, N. Flint, J. Molnos, M. Stieger, P. Caspers, M. Kamber, W. Keck, and K. E. Amrein.** 1999. Domain organization and molecular characterization of 13 two-component systems identified by genome sequencing of *Streptococcus pneumoniae*. Gene **237:**223–234.
34. **Letunic, I., R. R. Copley, B. Pils, S. Pinkert, J. Schultz, and P. Bork.** 2006. SMART 5: domains in the context of genomes and networks. Nucleic Acids Res. **34:**D257–D260.
35. **Livak, K. J., and T. D. Schmittgen.** 2001. Analysis of relative gene expression data using real-time quantitative PCR and the 2(-Delta Delta C(T)) method. Methods **25:**402–408.
36. **Martin, P. K., T. Li, D. Sun, D. P. Biek, and M. B. Schmid.** 1999. Role in cell permeability of an essential two-component system in *Staphylococcus aureus*. J. Bacteriol. **181:**3666–3673.
37. **Mohedano, M. L., K. Overweg, A. de la Fuente, M. Reuter, S. Altabe, F. Mulholland, D. de Mendoza, P. Lopez, and J. M. Wells.** 2005. Evidence that the essential response regulator YycF in *Streptococcus pneumoniae* modulates expression of fatty acid biosynthesis genes and alters membrane composition. J. Bacteriol. **187:**2357–2367.
38. **Msadek, T., V. Dartois, F. Kunst, M. L. Herbaud, F. Denizot, and G. Rapoport.** 1998. ClpP of *Bacillus subtilis* is required for competence development, motility, degradative enzyme synthesis, growth at high temperature and sporulation. Mol. Microbiol. **27:**899–914.
39. **Ng, W. L., K. M. Kazmierczak, and M. E. Winkler.** 2004. Defective cell wall synthesis in *Streptococcus pneumoniae* R6 depleted for the essential PcsB putative murein hydrolase or the VicR (YycF) response regulator. Mol. Microbiol. **53:**1161–1175.
40. **Ng, W. L., G. T. Robertson, K. M. Kazmierczak, J. Zhao, R. Gilmour, and M. E. Winkler.** 2003. Constitutive expression of PcsB suppresses the requirement for the essential VicR (YycF) response regulator in *Streptococcus pneumoniae* R6. Mol. Microbiol. **50:**1647–1663.
41. **Novick, R. P.** 2003. Autoinduction and signal transduction in the regulation of staphylococcal virulence. Mol. Microbiol. **48:**1429–1449.
42. **Oshida, T., M. Takano, M. Sugai, H. Suginaka, and T. Matsushita.** 1998. Expression analysis of the autolysin gene (*atl*) of *Staphylococcus aureus*. Microbiol. Immunol. **42:**655–659.
43. **Ramadurai, L., and R. K. Jayaswal.** 1997. Molecular cloning, sequencing, and expression of *lytM*, a unique autolytic gene of *Staphylococcus aureus*. J. Bacteriol. **179:**3625–3631.
44. **Raychaudhuri, D., and A. N. Chatterjee.** 1985. Use of resistant mutants to study the interaction of Triton X-100 with *Staphylococcus aureus*. J. Bacteriol. **164:**1337–1349.
45. **Reinscheid, D. J., B. Gottschalk, A. Schubert, B. J. Eikmanns, and G. S. Chhatwal.** 2001. Identification and molecular analysis of PcsB, a protein required for cell wall separation of group B *streptococcus*. J. Bacteriol. **183:**1175–1183.
46. **Rice, L. B.** 2006. Antimicrobial resistance in gram-positive bacteria. Am. J. Infect. Control **34:**S11–S19.
47. **Schneider, T. D., and R. M. Stephens.** 1990. Sequence logos: a new way to display consensus sequences. Nucleic Acids Res. **18:**6097–6100.
48. **Schultz, J., F. Milpetz, P. Bork, and C. P. Ponting.** 1998. SMART, a simple modular architecture research tool: identification of signaling domains. Proc. Natl. Acad. Sci. USA **95:**5857–5864.
49. **Senadheera, M. D., B. Guggenheim, G. A. Spatafora, Y. C. Huang, J. Choi, D. C. Hung, J. S. Treglown, S. D. Goodman, R. P. Ellen, and D. G. Cvitkovitch.** 2005. A VicRK signal transduction system in *Streptococcus mutans* affects *gtfBCD*, *gbpB*, and *ftf* expression; biofilm formation; and genetic competence development. J. Bacteriol. **187:**4064–4076.
50. **Smith, T. J., S. A. Blackman, and S. J. Foster.** 2000. Autolysins of *Bacillus subtilis*: multiple enzymes with multiple functions. Microbiology **146:**249–262.
51. **Sugai, M., T. Akiyama, H. Komatsuzawa, Y. Miyake, and H. Suginaka.** 1990. Characterization of sodium dodecyl sulfate-stable *Staphylococcus aureus* bacteriolytic enzymes by polyacrylamide gel electrophoresis. J. Bacteriol. **172:** 6494–6498.
52. **Sugai, M., H. Komatsuzawa, T. Akiyama, Y. M. Hong, T. Oshida, Y. Miyake, T. Yamaguchi, and H. Suginaka.** 1995. Identification of endo-beta-*N*-acetylglucosaminidase and *N*-acetylmuramyl-L-alanine amidase as cluster-dispersing enzymes in *Staphylococcus aureus*. J. Bacteriol. **177:**1491–1496.
53. **Takahashi, J., H. Komatsuzawa, S. Yamada, T. Nishida, H. Labischinski, T. Fujiwara, M. Ohara, J. Yamagishi, and M. Sugai.** 2002. Molecular characterization of an *atl* null mutant of *Staphylococcus aureus*. Microbiol. Immunol. **46:**601–612.
54. **Wagner, C., A. Saizieu Ad, H. J. Schonfeld, M. Kamber, R. Lange, C. J. Thompson, and M. G. Page.** 2002. Genetic analysis and functional characterization of the *Streptococcus pneumoniae vic* operon. Infect. Immun. **70:** 6121–6128.
55. **Wertheim, H. F., D. C. Melles, M. C. Vos, W. van Leeuwen, A. van Belkum, H. A. Verbrugh, and J. L. Nouwen.** 2005. The role of nasal carriage in *Staphylococcus aureus* infections. Lancet Infect. Dis. **5:**751–762.
56. **Yamada, S., M. Sugai, H. Komatsuzawa, S. Nakashima, T. Oshida, A. Matsumoto, and H. Suginaka.** 1996. An autolysin ring associated with cell separation of *Staphylococcus aureus*. J. Bacteriol. **178:**1565–1571.